Med Chem Res
DOI 10.1007/s00044-017-1903-0

MEDICINAL CHEMISTRY RESEARCH

ORIGINAL RESEARCH

Replacing triazole with diazole to optimize physicochemical properties of a click-based lead compound

Yinping Tian[1,2] · Wenhui Lv[1] · Qiuyue Meng[1] · Xuewei Li[1] · Wei Zeng[1] · Yaxin Lu[1] · Peng G. Wang[1,2] · Jin Jin[1] · Jie Shen[1]

Received: 20 February 2017 / Accepted: 17 April 2017

Abstract This work mainly demonstrated how the physicochemical properties of a click-based lead compound would be affected by the replacement of its triazole ring with a pyrazole or an imidazole ring. Compound **A1**, a click-based lead from our previous work, was a selective and moderate inhibitor against VEGFR2. Eight new derivatives of **A1** were synthesized, from which a pyrazole derivative **B2** was selected as a new lead. **B2** maintained the in vitro activity of **A1**. The solubilities of **B2** at pH 2.0 and pH 7.4 were enhanced to 1310 and 1.7 μg/mL, respectively. Its log *D* value of 3.4 would favor **B2** to be modified with hydrophilic fragments to further improve intestinal solubility in our future work.

Keywords Click chemistry · Lead optimization · Pyrazole · Imidazole · VEGFR2

Electronic supplementary material The online version of this article (doi:10.1007/s00044-017-1903-0) contains supplementary material, which is available to authorized users.

✉ Jin Jin
jinj@nankai.edu.cn

✉ Jie Shen
jieshen@nankai.edu.cn

[1] College of Pharmacy, Tianjin Key Laboratory of Molecular Drug Research, Nankai University, Haihe Education Park, 38 Tongyan Road, Tianjin 300353, China

[2] State Key Laboratory of Medicinal Chemical Biology, College of Pharmacy and Tianjin Key Laboratory of Molecular Drug Research, Nankai University, Haihe Education Park, 38 Tongyan Road, Tianjin 300353, China

Introduction

Since defined as a prototype click reaction in 2001 (Kolb et al. 2001; Tornøe et al. 2002), the Cu(I)-catalyzed Huisgen cycloaddition reaction has been widely used in medicinal chemistry to offer a growing library of click-based lead compounds (Thirumurugan et al. 2013). In our hands (Hou et al. 2011; Hou et al. 2012; Gu et al. 2012; Tian et al. 2016), such compounds are frequently poor in physicochemical (PC) properties, which should be partially related to the PC properties of the triazole ring: (i) the triazole ring is highly polarized and its topological polar surface area (*t*PSA) is 28 $Å^2$; (ii) the triazole ring is hardly protonated in vivo since its *p*Ka is less than 1; (iii) intermolecular CH•••N interactions can occur in some triazole compounds (Huang et al. 2010), presumably originated from the enhanced electronegativity of the involved C atoms of or near the triazole ring (Supplementary Fig. S1). The high *t*PSA value of the triazole fragment tends to disfavor the triazole compounds' cell permeability. Moreover, since the triazole ring is hardly protonated in water and can form intermolecular CH•••N interactions, the triazole compounds tend to have poor solubility. In Biopharmaceutical Classification System (Lindenberga et al. 2004), Class IV drugs that have low permeability and poor solubility are most challenging for oral administration. The triazole ring and diazole ring are greatly different in PC properties (Supplementary Scheme S1). Therefore, replacing the triazole ring of a click-based lead compound with a diazole ring might optimize the PC properties.

As an initial investigation to verify the above assumption, presented herein were our recent studies using nine compounds: three triazole compounds **A1–A3**, the corresponding pyrazole derivatives **B1–B3**, and the corresponding imidazole derivatives **C1–C3** (Fig. 1). The parent

Published online: 09 May 2017

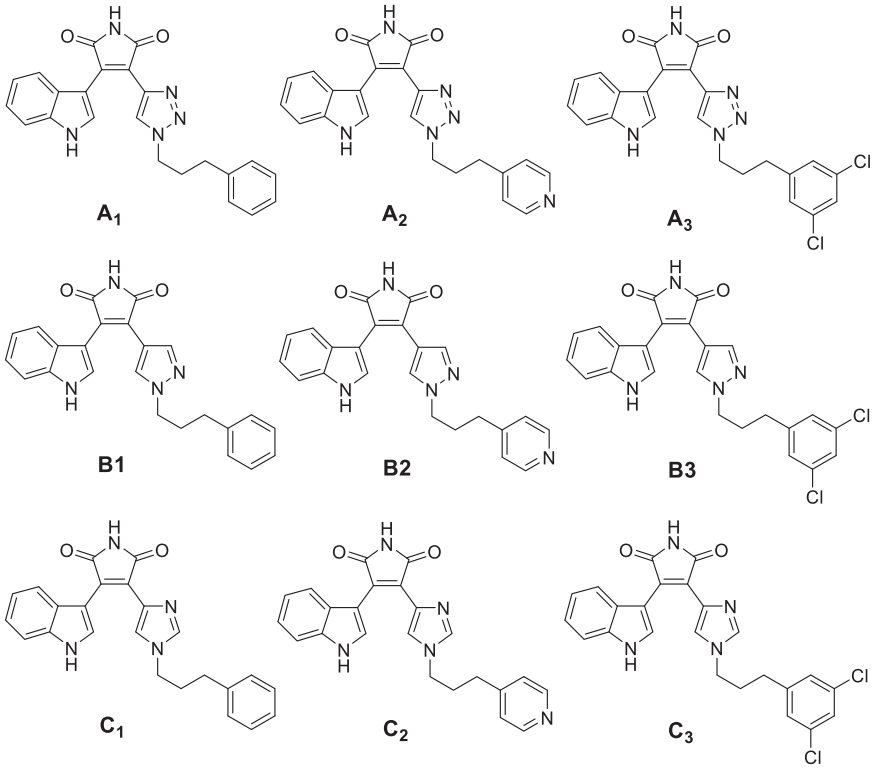

Fig. 1 Structures of target molecules

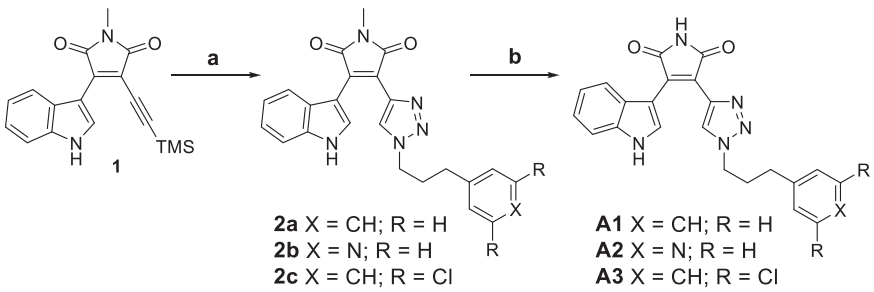

Scheme 1 *Reagents and conditions*: **a** CuF_2, R-N_3, microwave, 120 °C, 25–47%; **b** (i) KOH, EtOH, 85 °C, (ii) NH_4OAc, DMF, 140 °C, 14–35% for two steps

compound **A1** is a click-based lead compound from our previous work (Gu et al. 2012). It is a moderate and selective kinase inhibitor against VEGFR2, which is a well-established chemotherapy target (Musumeci et al. 2012). Compounds **A1**, **A2**, and **A3** are different in the terminal aromatic ring fragment to adjust the PC properties so as to help depict the effects of the triazole/diazole replacement on different types of compounds.

Material and methods

Chemistry

The general synthetic strategy for the triazole compounds is outlined in Scheme 1. For unknown reasons, the terminal alkyne from the desilylation of precursor **1** was unstable, which slowly turned into black at room temperature. In this regard, cupric fluoride was utilized to accomplish the desilylation and cycloaddition reaction in a one-pot two-stage procedure (Friscourt and Boons 2010). The triazole intermediates **2a–2c** were then sequentially treated with aqueous KOH solution and HCl solution to afford the corresponding anhydride intermediates, which were then heated with ammonium acetate to give the target compounds **A1–A3**.

The synthesis of **B1** and **B3** started with the *N*-alkylation of the pyrazole-4-boronic acid pinacol ester **3** to afford borate **4a** and **4b**. They were then reacted with the chloride **5** (Gu et al. 2012) to provide Suzuki coupling products **6a** and **6b**. Finally, treatment of **6a** and **6b** with KOH and ammonium acetate afforded **B1** and **B3** (Scheme 2). Due to the failure in the initial *N*-alkylation step, a different synthetic route was utilized to synthesize **B2** (Scheme 3).

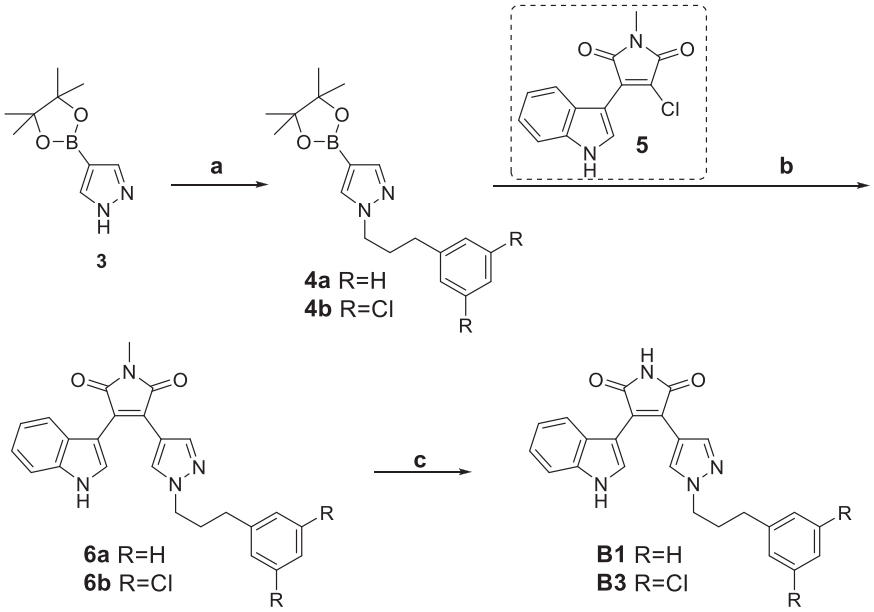

Scheme 2 *Reagents and conditions*: **a** (3-bromopropyl) benzene or 1,3-dichloro-5-(3-chloropropyl) benzene, Cs_2CO_3, DMF, rt, 60–74%; **b** $Pd(PPh_3)_4$, K_2CO_3, 1,4-dioxane, reflux, 40–90%; **c** (i) KOH, EtOH, 85 °C, (ii) NH_4OAc, DMF, 140 °C, 42–43% for two steps

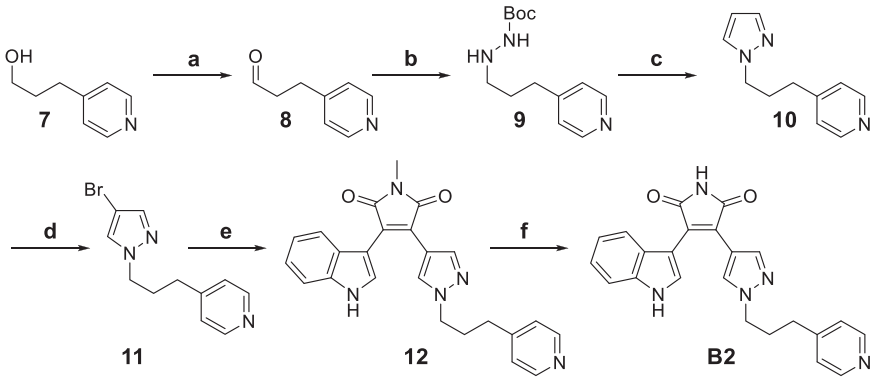

Scheme 3 *Reagents and conditions*: **a** $(COCl)_2$, DMSO, Et_3N, DCM, −60 °C, 63%; **b** (i) *i*-PrOH, reflux, *t*-BuOCONHNH$_2$, (ii) $NaBH_3CN$, *p*-$CH_3C_6H_4SO_3H$, MeOH, rt, 91% for two step; **c** 10 M HCl, 1,1,3,3-tetramethoxypropane, EtOH, reflux, 59%; **d** NBS, CH_3CN, reflux, 93%; **e** (i) Bis(pinacolato) diboron, $Pd(dppf)_2Cl_2$, KOAc, DMF, 80 °C, (ii) **5**, $Pd(PPh_3)_4$, K_2CO_3, DMF, 80 °C, 26% for two steps; **f** (i) KOH, EtOH, 85 °C, (ii) NH_4OAc, DMF, 140 °C, 26% for two steps

Swern oxidation followed by reductive amination of the commercially available compound **7** afforded the Boc-protected hydrazine derivative **9**. After the Boc-deprotection, it was coupled with 1,1,3,3-tetramethoxypropane to afford the pyrazole derivative **10**. Bromination of the compound **10** with NBS afforded the bromide **11**. A one-pot manipulation, including a Pd-catalyzed borylation reaction and a Suzuki coupling reaction with the chloride **5**, converted the bromide **11** into the intermediate **12**. Finally, **B2** was prepared by the treatment of **12** with KOH and ammonium acetate.

The syntheses of **C1–C3** (Scheme 4) started with the alkylation reactions of 2-(1*H*-imidazol-4-yl)acetonitrile **13** to provide intermediates **15a–15c**, which were hydrolyzed to the acetamide **16a–16c**. Condensation of **16a–16c** with indole-3-glyoxylic methyl ester **17** in the presence of *t*-BuOK gave target compounds **C1–C3**.

PC and pharmacodynamics (PD) studies

All the synthesized target compounds were preliminarily investigated for their PC and PD properties. First, solubility and partipation coefficient (log*D*) were experimentally determined. Since compounds **B2** and **C2** showed the most favorable PC properties, they were selected in the follwing in vitro PD studies, along with the initial lead compound **A1** for comparison. Bovine aortic endothelial cells (BEACs) were employed in both MTT test and wound-healing assay (Denker and Barber 2002) to evaluate the cytotoxicity and migration-inhibitory activity, respectively.

Results and discussion

Diazole compounds were more water soluble than the corresponding triazole compounds (Table 1). Compounds **A1**,

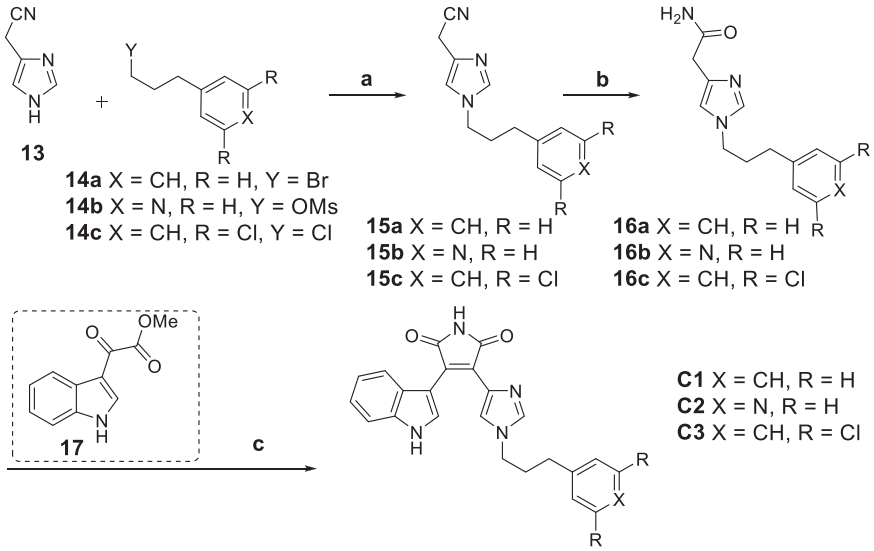

Scheme 4 *Reagents and conditions*: **a** Cs_2CO_3, DMF, rt, 22–72%; **b** K_2CO_3, H_2O_2, DMSO/H_2O, 0 °C rt, 51–57%; **c** *t*-BuOK, DMF, rt, 22–54%

Table 1 Solubility and log *D* data

Compounds	Solubility (μg/mL)		log *D*	PSA (Å^2)[a]
	pH = 2.0	pH = 7.4		
A1	<0.1	<0.1	3.7	86
B1	<0.1	<0.1	4.4	74
C1	13.3	<0.1	3.8	74
A2	498	<0.1	2.5	99
B2	1310	1.7	3.4	86
C2	1990	1.8	2.3	86
A3	<0.1	<0.1	4.3	86
B3	<0.1	<0.1	6.1	74
C3	3.5	<0.1	3.9	74

Note: Mean of three independent triplicate experiments

[a] Calculated values of ChemOffice (2015)

Table 2 In vitro PD data

Compounds	Toxicity assays	Activity assays	
	MTT assay: cell growth inhibition at 2 μm (%)	Wound-healing assay: cell migration rate at 1 μM (%)	VEGFR2 inhibition assay: IC_{50} (μM)[a]
A1	9 ± 7	69 ± 10	0.20
B2	19 ± 4	41 ± 10	0.18
C2	18 ± 9	48 ± 7	1.25
Sunitinib	28 ± 6	38 ± 9	0.08[b]
Staurosporine	n.d.[c]	n.d.[c]	0.006
Negative control	n.d.[c]	77 ± 10	n.d.[c]

Note: Mean of three independent triplicate experiments

[a] VEGFR2 inhibition was determined at six different inhibitor concentrations

[b] Sun et al. (2003)

[c] n.d. = not determined

B1, **C1**, **A3**, **B3**, and **C3** all had low solubilities, indicating that the triazole/diazole replacement alone could not completely overcome the solubility problem for compounds with extremely low solubility. Compounds **A2**, **B2**, and **C2** all contained a hydrophilic pyridine ring fragment. Their solublilites at pH 2.0 were above 0.5 mg/mL, and their solubilities at pH 7.4 were all below 2 μg/mL. These results implied that their in vivo dissociation rates might be acceptable in the stomach, but not satisfactory in the intestine. Therefore, it should be necessary in our future work to modify their structures with additional polar fragments. As for the log *D* values, the following general trend was observed: pyrazole > imidazole ≈ triazole. The pyrazole ring is less polar than the triazole ring, and less protonated than the imidazole ring. These facts well explain why the pyrazole compound has the largest log *D* value.

In MTT test, 2 μM concentration of **A1**, **B2**, and **C2** all showed low toxicities so as to inhibit BEACs growth by 9, 19, and 18%, respectively. **A1**, **B2**, and **C2** at 1 μM concentration were screened in wound-healing assay, cell migration rates were 69, 41, and 48%, respectively, as compared with 77% migration rate in the negative control. That is, whereas **B2** and **C2** were slightly more toxic than **A1**, they were dramatically more active than **A1** in inhibiting cell migration. Unlike the similar potencies in cell-based experiments, the IC_{50} values of **B2** and **C2** against VEGFR2 were 0.18 and 1.25 μM, respectively. That is, only **B2** maintained the inhibitory capacity of **A1** against VEGFR2 enzyme (Table 2). It might be attributed to the different localizations of N atoms, which might interact with VEGFR2 protein in the binding complex.

Conclusion

"In the future, 'drugability' screening may precede biological receptor activity screening". Dr. C.A. Lipinski made this statement to emphasize the importance of PK property evaluations in the early stage of drug discovery (Lipinski 2000). In this paper, we present the triazole/diazole replacement to adjust the PC properties of click-based lead compounds. The pyrazole derivative **B2** is our newly identified lead compound. Compared with the triazole compound **A1**, while **B2** maintains similar PD properties, its solubility is dramatically enhanced. Additionally, its log *D* value of 3.4, as well as its decreased *t*PSA value, positions **B2** advantageously for being modified with hydrophilic fragments to further improve the intestinal solubility in our future work.

Experimental

Chemistry

Reagents and solvents were purchased from Alfa Aesar and used without further purification. Thin-layer chromatography (TLC) was carried out on silica GF254 plates (Qingdao). Column chromatography was performed on silica gel (200–300 mesh normal phase from Qingdao, or 200–400 mesh reverse phase from MED). 1H and 13C NMR spectra were obtained on a Bruker Advance 400 spectrometer, using tetramethylsilane as an internal standard. High-resolution mass spectra (HRMS) were obtained on a QFT–ESI mass spectrometer. Sunitinib and staurosporine were purchased from MedChem Express (Shanghai) Technology Corporation and was employed as the standard compound in bioassays.

The synthesis of compounds **1**, **2**, **4**, **5**, **6**, **8**, **9**, **10**, **11**, **12**, **14**, **15**, **16**, and **17** was described in Supplementary Material.

*General procedure for the synthesis of target molecules **A1–A3** and **B1–B3***

To a solution of compounds **2**, **6**, or **12** (1 equiv.) in EtOH (8 mL) was added 5 M KOH aqueous solution (2 mL) and the resulting mixture was stirred at 85 °C for 8 h. Then the mixture was cooled to room temperature and was neutralized with 2 M HCl aqueous solution. After extraction with ethyl actate (three times), the organic layers were dried and concentrated to give the crude anhydride intermediate. To a solution of this crude anhydride in DMF (20 mL) was added ammonium acetate (80 equiv.) and the mixture was heated to 140 °C for 8 h. The resulting mixture was concentrated in vacuo, the residue was dissolved in ethyl acetate and washed twice with saturated solution of $NaHCO_3$. The organic layer was dried, concentrated in vacuo, and the residue was purified by column chromatography on silica gel eluted with DCM/MeOH (50:1–10:1) to give compounds **A1–A3** and **B1–B3**.

Compound **A1** was synthesized via the reported procedures (Gu et al. 2012). The NMR data were consistent with those reported. ^{1}H NMR (400 MHz, DMSO-d_6) δ 2.15 (2H, m, $\underline{CH_2}CH_2Ph$), 2.56 (2H, t, $J = 7.6$ Hz, $CH_2\underline{CH_2}Ph$), 4.45 (2H, t, $J = 7.2$ Hz, $N\underline{CH_2}$), 6.82–6.88 (2H, m, Ar-H), 7.08–7.12 (1H, m, Ar-H), 7.18–7.21 (3H, m, Ar-H), 7.28–7.31 (2H, m, Ar-H), 7.45 (1H, d, $J = 8.0$ Hz, H-14), 8.16 (1H, d, $J = 2.8$ Hz, H-13), 8.50 (1H, s, H-18), 11.10 (1H, s, $CO\underline{NH}CO$), 11.89 (1H, d, $J = 2.0$ Hz, NH).

3-(1H-indol-3-yl)-4-(1-(3-(pyridin-4-yl)propyl)-1H-1,2,3-triazol-4-yl)-1H-pyrrole-2,5-dione (**A2**) Yield 35%; a yellow solid. ^{1}H NMR (400 MHz, DMSO-d_6) δ 2.18 (2H, m, $\underline{CH_2}CH_2Py$), 2.58 (2H, t, $J = 7.8$ Hz, $CH_2\underline{CH_2}Py$), 4.46 (2H, t, $J = 6.8$ Hz, $N\underline{CH_2}$), 6.82–6.88 (2H, m, Ar-H), 7.08–7.12 (1H, m, Ar-H), 7.22 (2H, d, $J = 5.6$ Hz, Ar-H), 7.45 (1H, d, $J = 8.0$ Hz, H-14), 8.16 (1H, d, $J = 2.4$ Hz, H-13), 8.46 (2H, d, $J = 6.0$ Hz, Py-$\underline{CH}N\underline{CH}$), 8.51 (1H, s, H-18), 11.11 (1H, s, $CO\underline{NH}CO$), 11.90 (1H, s, NH). ^{13}C NMR (100 MHz, DMSO-d_6) δ 30.6 ($\underline{CH_2}CH_2Py$), 31.4 ($CH_2\underline{CH_2}Py$), 49.3 ($N\underline{CH_2}$), 105.1 (C-8), 112.5 (C-17), 120.2, 121.2, 122.0, 122.4, 124.4, 125.6, 126.3, 132.2, 133.0, 136.9, 137.4, 150.0 (Py-$\underline{CH}N\underline{CH}$), 150.1 (Py-$\underline{CH}N\underline{CH}$), 172.4 (C=O), 171.6 (C=O). HRMS (MALDI) Calcd. for $C_{22}H_{18}N_6O_2$ $[M+Na]^+$ 421.1383; found, 421.1378.

3-(1-(3-(3,5-dichlorophenyl)propyl)-1H-1,2,3-triazol-4-yl)-4-(1H-indol-3-yl)-1H-pyrrole-2,5-dione (**A3**) Yield 14%; a yellow solid. ^{1}H NMR (400 MHz, DMSO-d_6) δ 2.21 (2H, m, $\underline{CH_2}CH_2Ph$), 2.63 (2H, t, $J = 7.6$ Hz, $CH_2\underline{CH_2}Ph$), 4.48 (2H, t, $J = 6.8$ Hz, $N\underline{CH_2}$), 6.88–6.94 (2H, m, Ar-H), 7.15 (1H, t, $J = 7.4$ Hz, Ar-H), 7.33 (2H, d, $J = 1.6$ Hz, Ar-H), 7.45 (1H, d, $J = 1.8$ Hz, Ar-H), 7.50 (1H, d, $J = 8.0$ Hz, H-14), 8.21 (1H, d, $J = 2.4$ Hz, H-13), 8.55 (1H, s, H-18), 11.15 (1H, s, $CO\underline{NH}CO$), 11.95 (1H, s, NH). ^{13}C NMR (100 MHz, DMSO-d_6) δ 31.1 ($\underline{CH_2}CH_2Ph$), 31.6 ($CH_2\underline{CH_2}Ph$), 49.3 ($N\underline{CH_2}$), 105.1 (C-8), 112.5 (C-17), 120.2, 121.2, 122.0, 122.3, 125.6, 126.2, 126.3, 127.8, 132.2, 133.0, 134.4, 136.9, 137.4, 145.6, 172.4 (C=O), 172.6 (C=O). HRMS (MALDI) Calcd. for $C_{23}H_{17}Cl_2N_5O_2$ $[M+Na]^+$ 488.0652; found, 488.0658.

3-(1H-indol-3-yl)-4-(1-(3-phenylpropyl)-1H-pyrazol-4-yl)-1H-pyrrole-2,5-dione (**B1**) Yield 42%; a yellow solid. ^{1}H NMR (400 MHz, DMSO-d_6) δ 2.00 (2H, m, $\underline{CH_2}CH_2Ph$), 2.48 (2H, buried t, $J = 8.0$ Hz, $CH_2\underline{CH_2}Ph$), 4.08 (2H, t, $J = 6.8$ Hz, $N\underline{CH_2}$), 6.84 (1H, d, $J = 8.4$ Hz, Ar-H), 6.90

(1H, t, $J = 7.6$ Hz, Ar-H), 7.12–7.20 (4H, m, Ar-H), 7.28 (2H, t, $J = 7.6$ Hz, Ar-H), 7.51 (2H, m, H-14 and H-21), 7.81 (1H, d, $J = 2.8$ Hz, H-13), 8.00 (1H, s, H-18), 10.97 (1H, s, CONHCO), 11.86 (1H, d, $J = 2.0$ Hz, NH). ^{13}C NMR (100 MHz, DMSO-d_6) δ 31.3 ($\underline{CH_2}CH_2Ph$), 31.8 ($CH_2\underline{CH_2}Ph$), 50.7 ($N\underline{CH_2}$), 103.9 (C-8), 110.6 (C-9), 112.3 (C-17), 119.5, 121.2, 121.8, 123.8, 124.8, 125.9, 127.5, 128.2, 128.3, 129.4, 131.0, 136.4, 139.2, 141.0, 172.6 (C=O), 172.6 (C=O). HRMS (MALDI) Calcd. for $C_{24}H_{20}N_4O_2$ $[M+H]^+$ 397.1659; found, 397.1659.

3-(1H-indol-3-yl)-4-(1-(3-(pyridin-4-yl)propyl)-1H-pyrazol-4-yl)-1H-pyrrole-2,5-dione (**B2**) Yield 27%, a yellow solid. ^{1}H NMR (400 MHz, DMSO-d_6) δ 2.03 (2H, m, $\underline{CH_2}CH_2Py$), 2.48 (2H, buried t, $CH_2\underline{CH_2}Py$), 4.10 (2H, t, $J = 6.6$ Hz, $N\underline{CH_2}$), 6.84–6.92 (2H, m, Ar-H), 7.12–7.18 (3H, m, Ar-H), 7.50–7.52 (2H, m, H-14 and H-21), 7.82 (1H, d, $J = 2.4$ Hz, H-13), 7.95 (1H, s, H-18), 8.28–8.62 (2H, m, Py-$\underline{CH}NCH$), 10.95 (1H, s, CONHCO), 11.85 (1H, s, NH). ^{13}C NMR (100 MHz, DMSO-d_6) δ 30.6 ($\underline{CH_2}CH_2Py$), 31.5 ($CH_2\underline{CH_2}Py$), 51.1 ($N\underline{CH_2}$), 104.4 (C-8), 111.2 (C-9), 112.8 (C-17), 120.0, 121.7, 122.2, 124.3, 125.3, 128.1, 129.9, 131.5, 136.9, 139.8, 149.9 (Py-CHN$\underline{CH}$), 150.5 (Py-$\underline{CH}$NCH), 173.1 (C=O), 173.1 (C=O). HRMS (MALDI) Calcd. for $C_{23}H_{19}N_5O_2$ $[M+Na]^+$ 398.1612; found, 398.1615.

3-(1-(3-(3,5-dichlorophenyl)propyl)-1H-pyrazol-4-yl)-4-(1H-indol-3-yl)-1H-pyrrole-2,5-dione (**B3**) Yield 43%; a yellow solid. ^{1}H NMR (400 MHz, DMSO-d_6) δ 2.02 (2H, m, $\underline{CH_2}CH_2Ph$), 2.51 (2H, buried t, $CH_2\underline{CH_2}Ph$), 4.09 (2H, t, $J = 7.2$ Hz, $N\underline{CH_2}$), 6.85 (1H, d, $J = 8.0$ Hz, Ar-H), 6.91 (1H, t, $J = 7.4$ Hz, Ar-H), 7.15 (1H, t, $J = 7.2$ Hz, Ar-H), 7.23 (2H, d, $J = 1.6$ Hz, Ar-H), 7.42 (1H, d, $J = 1.6$ Hz, Ar-H), 7.51–7.53 (2H, m, H-14 and H-21), 7.82 (1H, d, $J = 2.8$ Hz, H-13), 7.96 (1H, s, H-18), 10.95 (1H, s, CONHCO), 11.85 (1H, s, NH). ^{13}C NMR (100 MHz, DMSO-d_6) δ 31.2 ($\underline{CH_2}CH_2Ph$), 31.7 ($CH_2\underline{CH_2}Ph$), 51.0 ($N\underline{CH_2}$), 104.4 (C-8), 111.2 (C-9), 112.8 (C-17), 120.0, 121.7, 122.2, 124.4, 125.3, 126.1, 127.7, 128.1, 129.9, 131.5, 134.3, 137.0, 139.7, 146.0, 173.1 (C=O), 173.1 (C=O). HRMS (MALDI) Calcd. for $C_{24}H_{18}Cl_2N_4O_2$ $[M+Na]^+$ 487.0699; found, 487.0694.

General procedure for the synthesis of target molecules ***C1–C3***

1M *t*-BuOK in THF (5 mL) was added to a mixture of compoud **16** (1 equiv.), compound **17** (2 equiv.), and 4 Å molecular sieve (100 mg) in anhydrous DMF (10 mL) at 0 °C under N_2 atmosphere, the whole solution was stirred at room temperatue for 24 h. After the completion of the reaction (monitored by TLC), the resulting solution was filtered and concentrated in vacuo. The residue was dissolved in ethyl acetate and washed twice with saturated solution of NH_4Cl. The organic layer was dried, concentrated in vacuo, and the residue was purified by column chromatography on silica gel eluted with DCM/MeOH (25:1–10:1) to give compounds **C1–C3**.

3-(1H-indol-3-yl)-4-(1-(3-phenylpropyl)-1H-imidazol-4-yl)-1H-pyrrole-2,5-dione (**C1**) Yield 31%, a yellow solid. ^{1}H NMR (400 MHz, DMSO-d_6) δ 2.07 (2H, m, $\underline{CH_2}CH_2Ph$), 2.54 (2H, buried t, $J = 8.0$ Hz, $CH_2\underline{CH_2}Ph$), 4.06 (2H, t, $J = 6.8$ Hz, $N\underline{CH_2}$), 6.86 (1H, t, $J = 7.6$ Hz, Ar-H), 7.09 (2H, t, $J = 7.2$ Hz, Ar-H), 7.21 (3H, d, $J = 7.2$ Hz, Ar-H), 7.30 (2H, t, $J = 7.2$ Hz, Ar-H), 7.42 (1H, d, $J = 8.0$ Hz, Ar-H), 7.69 (1H, s, Ar-H), 7.80 (1H, s, H-20), 8.07 (1H, d, $J = 2.4$ Hz, H-13), 10.90 (1H, s, CONHCO), 11.69 (1H, s, NH). ^{13}C NMR (100 MHz, DMSO-d_6) δ 32.4 ($\underline{CH_2}CH_2Ph$), 32.6 ($CH_2\underline{CH_2}Ph$), 46.4 ($N\underline{CH_2}$), 105.5 (C-8), 112.1 (C-17), 119.7, 121.9, 122.3, 123.2, 126.1, 126.4, 126.4, 128.7, 128.8, 129.2, 131.1, 131.9, 136.6, 138.4, 141.4 (C-25), 173.1 (C=O), 173.3 (C=O). HRMS (MALDI) Calcd. for $C_{24}H_{20}N_4O_2$ $[M+Na]^+$ 397.1659; found, 397.1656.

3-(1H-indol-3-yl)-4-(1-(3-(pyridin-4-yl)propyl)-1H-imidazol-4-yl)-1H-pyrrole-2,5-dione (**C2**) Yield 22%, a yellow solid. ^{1}H NMR (400 MHz, DMSO-d_6) δ 2.07 (2H, m, $\underline{CH_2}CH_2Py$), 2.55 (2H, t, $J = 7.4$ Hz, $CH_2\underline{CH_2}Py$), 4.05 (2H, t, $J = 7.2$ Hz, $N\underline{CH_2}$), 6.85 (1H, t, $J = 7.6$ Hz, Ar-H), 7.12–7.00 (2H, m, Ar-H), 7.22 (2H, d, $J = 5.6$ Hz, Ar-H), 7.40 (1H, d, $J = 8.1$ Hz, Ar-H), 7.68 (1H, s, Ar-H), 7.78 (1H, s, H-20), 8.05 (1H, d, $J = 2.6$ Hz, H-13), 8.46 (2H, d, $J = 5.7$ Hz, Py-$\underline{CH}NCH$), 10.85 (1H, s, CONHCO), 11.64 (1H, s, NH). ^{13}C NMR (100 MHz, DMSO-d_6) δ 31.3 ($\underline{CH_2}CH_2Py$), 31.6 ($CH_2\underline{CH_2}Py$), 46.3 ($N\underline{CH_2}$), 105.5 (C-8), 112.1 (C-17), 119.7, 121.9, 122.3, 123.2, 124.3, 126.1, 126.4, 129.2, 131.1, 131.9, 136.6, 138.4, 150.0 (Py-CHN$\underline{CH}$), 150.3 (Py-$\underline{CH}$NCH), 173.1 (C=O), 173.3 (C=O). HRMS (MALDI) Calcd. for $C_{23}H_{19}N_5O_2$ $[M+H]^+$ 398.1612; found, 398.1609.

3-(1-(3-(3,5-dichlorophenyl)propyl)-1H-imidazol-4-yl)-4-(1H-indol-3-yl)-1H-pyrrole-2,5-dione (**C3**) Yield 54%, a yellow solid. ^{1}H NMR (400 MHz, DMSO-d_6) δ 2.07 (2H, m, $\underline{CH_2}CH_2Ph$), 2.58 (2H, t, $J = 7.4$ Hz, $CH_2\underline{CH_2}Ph$), 4.04 (2H, t, $J = 6.8$ Hz, $N\underline{CH_2}$), 6.86 (1H, t, $J = 7.6$ Hz, Ar-H), 7.06–7.11 (2H, m, Ar-H), 7.29 (2H, d, $J = 1.6$ Hz, Ar-H), 7.41–7.43 (2H, m, Ar-H), 7.68 (1H, s, Ar-H), 7.78 (1H, s, H-20), 8.06 (1H, d, $J = 2.4$ Hz, H-13), 10.86 (1H, s, CONHCO), 11.66 (1H, s, NH). ^{13}C NMR (100 MHz, DMSO-d_6) δ 31.8 ($\underline{CH_2}CH_2Ph$), 31.9 ($CH_2\underline{CH_2}Ph$), 46.3 ($N\underline{CH_2}$), 105.5 (C-8), 112.1 (C-17), 119.7, 121.9, 122.3, 123.2, 126.1, 126.2, 126.4, 127.6, 129.2, 131.1, 131.9,

134.4, 136.6, 138.3, 145.9, 173.1 (C=O), 173.2 (C=O). HRMS (MALDI) Calcd. for $C_{24}H_{18}Cl_2N_4O_2$ $[M+Na]^+$ 487.0699; found, 487.0697.

PC and PD studies

PC data determination

Procedure for solubility determination Excess amounts of the test compounds were placed in screw-capped vials containing 500 μL of PBS (0.2 M NaH_2PO_4-NaOH in water, pH = 2.0 or 7.4). The suspensions were vortexed for 2 min and kept in a shaker with 160 rpm maintained at 25 °C for 24 h. After centrifugation at 10,000 rpm for 10 min, the filtrates were analyzed by Dionex U-3000, Venusil MP C18, 4.6*150 mm, 5 μM, 100 Å HPLC (High-performance liquid chromatography).

Procedure for log D determination Weighed amounts (200 μg) of the test compounds in PBS (500 μL, 0.2 M NaH_2PO_4-NaOH in water, pH = 7.4) and Octanol (500 μL) were shaken with 160 rpm at 37 °C for 1 h to reach equilibrium. Then the two phases were separated by centrifugation at 10,000 rpm for 10 min. The concentrations of the test compounds in the Octanol and the PBS layer were determined by HPLC. The log *D* was calculated by employing the following equation: $\log D = \log (AUC_{OCT}/AUC_{PBS})$. AUC_{OCT} and AUC_{PBS} were the UV absorption areas for octanol and the PBS layer.

Biological data determination

VEGFR2 inhibition assays The assays were performed on a 384-well plate. To each well were sequentially added three solutions in kinase base buffer (50 mM HEPES at pH 7.5, 0.0015% Brij-35, 10 mM $MgCl_2$, 2 mM DTT): (1) 5 μL 5× inhibitor solution containing 2% DMSO; (2) 10 μL 2.5× VEGFR solution; (3) 10 μL 2.5× ATP and FAM-labeled fluorogenic peptide substrate solution (5-FAM-EEPLYWSFPAKK K-$CONH_2$). As a result, the final volume of the solution in each well was 25 μL, and it contained an inhibitor at the designed concentration, 92 μM ATP, 3 μM peptide substrate and 1.2 nM VEGFR2. The assay plate was incubated at 28 °C for 1 h. Assays were stopped by adding 25 μL stop buffer (100 mM HEPES at pH 7.5, 0.015% Brij-35, 0.2% coating reagent #3, 50 mM EDTA) and the data were collected on Caliper EZ-reader.

MTT assay BEACs were treated with each compound (**A1**, **B2**, **C2**, and sunitinib) at designed concentration (2 μM) for 48 h followed by the addition of MTT to each well. Further cultured for 4 h, the supernatant was removed and DMSO was added. The absorption value of each well at 570 nm was measured by using a microplate reader (cell viability was normalized by the absorbance of untreated cells).

Wound-healing assay BAECs were plated in 6-well plates (2×10^5/well) to form a confluent monolayer. The wound was created by manually scraping the well with a sterile 200 μL pipette tip. The supernatant was washed followed by the addition of compound solution to a final concentration of 1 μM, respectively. VEGF (10 ng/mL) were added to each well except for the untreated control. Images of the wound-healing at 0 h and 16 h were captured, respectively, in the same scratched area by using an Olympus microscope and quantified by measuring the distance across the wound area with Image J software. Cell migration was presented as the percentage of wound closure as follow: wound closure % = [1-(wound distance at 16 h/wound distance at 0 h)] × 100. In negitve control, experimental procedure was the same procedure except for the addition of compound solution.

Acknowledgements This study was supported by National Natural Science Foundation of China (No. 21272127) and Natural Science Foundation of Tianjin, China (No. 16JCQNJC13500).

Compliance with ethical standards

Conflict of interest The authors declare that they have no competing interests.

References

Denker SP, Barber DL (2002) Cell migration requires both ion translocation and cytoskeletal anchoring by the Na-H exchanger NHE1. J Cell Biol 159:1087–1096

Friscourt F, Boons GJ (2010) One-pot three-step synthesis of 1,2,3-triazoles by copper-catalyzed cycloaddition of azides with alkynes formed by a sonogashira cross-coupling and desilylation. Org Let 12:4936–4939

Gu G, Wang H, Liu P, Fu C, Li Z, Cao X, Li Y, Fang Q, Xu F, Shen J, Wang PG (2012) Discovery and structural insight of a highly selective protein kinase inhibitor hit through click chemistry. Chem Commun 48:2788–2790

Huang CC, Wu FL, Lo YH, Lai WR, Lin CH (2010) Methyl 1-benzyl-1H-1,2,3-triazole-4-carboxylate. Acta Cryst E66:O1690

Hou J, Feng C, Li Z, Fang Q, Wang H, Gu G, Shi Y, Liu P, Xu F, Yin Z, Shen J, Wang P (2011) Structure-based optimization of click-based histone deacetylase inhibitors. Eur J Med Chem 46:3190–3200

Hou J, Li Z, Fang Q, Feng C, Zhang H, Guo W, Wang H, Gu G, Tian Y, Liu P, Liu R, Lin J, Shi Y, Yin Z, Shen J, Wang P (2012) Discovery and extensive in vitro evaluations of NK-HDAC-1: a chiral histone deacetylase inhibitor as a promising lead. J Med Chem 55:3066–3075

Kolb HC, Fokin MG, Sharpless KB (2001) Click chemistry: diverse chemical function from a few good reactions. Angew Chem Int Ed 40:2004–2021

Lindenberga M, Koppb S, Dressmana JB (2004) Classification of orally administered drugs on the world health organization model list of essential medicines according to the biopharmaceutics classification system. Eur J Pharm Biopharm 58:265–278

Lipinski CA (2000) Drug-like properties and the causes of poor solubility and poor permeability. J Pharmacol Toxicol Methods 44:235–249

Musumeci F, Radi M, Brullo C, Schenone S (2012) Vascular endothelial growth factor (VEGF) receptors: drugs and new inhibitors. J Med Chem 55:10797–10822

Sun L, Liang C, Shirazian S, Zhou Y, Miller T, Cui J, Fukuda JY, Chu J, Nematalla A, Wang X, Chen H, Sistla A, Luu TC, Tang F, Wei J, Tang C (2003) Discovery of 5-[5-fluoro-2-oxo-1,2-dihydroindol-(3Z)-ylidenemethyl]-2,4-dimethyl-1H-pyrrole-3-carboxylic acid (2-diethylaminoethyl)amide, a novel tyrosine kinase inhibitor targeting vascular endothelial and platelet-derived growth factor receptor tyrosine kinase. J Med Chem 46:1116–1119

Thirumurugan P, Matosiuk D, Jozwiak K (2013) Click chemistry for drug development and diverse chemical-biology applications. Chem Rev 113:4905–4979

Tian Y, Jin J, Wang C, Lv W, Li X, Che X, Gong Y, Li Y, Li Q, Hou J, Wang PG, Shen J (2016) A sub-milligram-synthesis protocol for in vitro screening of HDAC11 inhibitors. Bioorg Med Chem Lett 26:2434–2437

Tornøe CW, Christensen C, Meldal M (2002) Peptidotriazoles on solid phase: [1,2,3]-triazoles by regiospecific copper(I)-catalyzed 1,3-dipolar cycloadditions of terminal alkynes to azides. J Org Chem 67:3057–3064